Sensors and Actuators B 193 (2014) 844–850

Contents lists available at ScienceDirect

Sensors and Actuators B: Chemical

journal homepage: www.elsevier.com/locate/snb

A molecularly imprinted electrochemical sensor based on sol–gel technology and multiwalled carbon nanotubes–Nafion functional layer for determination of 2-nonylphenol in environmental samples

Jin Zhang[a,b,*], Yanhui Niu[b], Shijie Li[a,*], Rongqin Luo[a], Chaoying Wang[b]

[a] State Key Laboratory of Environmental Geochemistry, Institute of Geochemistry, Chinese Academy of Sciences, Guiyang 550002, PR China
[b] School of Chemistry and Life Science, Guizhou Normal College, Guiyang 550018, PR China

ARTICLE INFO

Article history:
Received 6 August 2013
Received in revised form
19 November 2013
Accepted 24 November 2013
Available online 11 December 2013

Keywords:
Amperometric sensor
Imprinted sol–gel
Multiwalled carbon nanotubes
Nafion
2-Nonylphenol

ABSTRACT

In this work, we have proposed a sensitive and selective detection technique for 2-nonylphenol (2-NP) based on the differential pulse voltammetry at a molecularly imprinted film on a glassy carbon electrode (GCE). The imprinted film was immobilised on the GCE by electrodeposition of a molecularly imprinted polymer (MIP) sol–gel consisting of a multiwalled carbon nanotube (MWNT)–Nafion (NF) composite. The modification procedure was characterized by cyclic voltammetry (CV), electrochemical impedance spectroscopy (EIS) and scanning electron microscope (SEM). The recognition between MIP sol–gel film and target molecule was observed by measuring the change in DPV response of the oxidation-reduction probe, $K_3Fe(CN)_6$ on GCE. Under optimized operational conditions, a linear response was obtained covering the concentration range from 0.2 to 360 μmol L^{-1} with a detection limit of 0.06 μmol L^{-1}. The proposed sensor was applied to 2-NP determination in water and soil samples with the recoveries from 95.4 to 98.1%, showing a promising potential application in environment samples. Additionally, The imprinted sensor demonstrated higher affinity for target 2-NP than that of non-imprinted polymer (NIP) sensor.

1. Introduction

Nonylphenol (NP), the main biodegradation of nonylphenol ethoxylates and a toxic xenobiotic compound classified as an environmental endocrine disrupter, is widely used as a raw material in industrial activities [1,2]. Due to its high hydrophobicity and low degradation rates, NP shows a persistent condition in soil and sewage sludge [3]. Recently, NP has received a great deal of attention in environmental protection and its endocrine disrupting effect in the aquatic environment is particularly well documented [4]. Methods for NP determination have included spectrophotometry [5], solid-phase microextraction procedures [6], high performance liquid chromatography [7], gas chromatography-mass spectrometer [8] and biosensors [9,10]. Although spectrophotometry and chromatography have low detection limit and high sensitivity, they suffer from low selectivity, long analysis time intervals, expensive instruments and possible production of secondary toxic compounds [11]. The molecular recognition materials in biosensor, meanwhile, show intrinsic difficulties in practical applications, due to instability of biomolecules. Therefore, a novel and effective material for improving stability of sensor was needed.

Molecularly imprinted polymers (MIPs) have been considered as promising alternatives to biological molecules and applied as recognition elements in sensors [12]. Interest in MIP modified electrodes has surged owing to their high selectivity, chemical stability, moderate cost and easy preparation [13]. However, they often suffer from drawbacks such as low binding capacity resulting in a very weak electronic signal, slow binding kinetics leading to long analysis time and the reported difficulties related to the integration of the MIP with the transducer [14]. In order to enhance the chemosensor response, hybrid materials prepared with MIP and carbon nanotubes [15,16], enzyme [17] or metal nanoparticle composites [18,19] have been employed with the same purpose. Electropolymerization has several advantages over other preparation procedures of MIP hybrid materials films. In particular, an ultrathin polymeric film can be easily grown adherent to a conducting electrode of any shape and with a thickness controlled by the electrochemical parameters of the deposition [20]. This structure facilitates direct communication between the MIP film and the electrode surface, which can meet the sensor requirements of fast response and miniaturization [21].

Carbon nanotubes, mainly multiwalled carbon nanotubes (MWNT) with a high surface area, excellent electrical conductivity

* Corresponding authors. Tel.: +86 851 5816647; fax: +86 851 5816647.
E-mail addresses: jzhang@gznc.edu.cn (J. Zhang), lishijie@vip.gyig.ac.cn (S. Li).

0925-4005/$ – see front matter © 2013 Elsevier B.V. All rights reserved.
http://dx.doi.org/10.1016/j.snb.2013.11.081

and good thermal stability [22], have generated considerable interest in electrochemical sensors [23]. A major barrier for developing MWNT-based sensor is the insolubility of MWNT in many solvents [22]. To overcome this situation, Wang et al. reported on the ability of the widely used perfluorosulfonated polymer Nafion (NF), with unique ion-exchange, biocompatibility and thermal stability, as well as high conductivity [24], to solubilize MWNT and found that MWNT can be suspended in solutions of Nafion in a phosphate buffer or alcohol [25]. Sol–gel imprinting process is a promising way to improve the performance of MIP film via forming a sol–gel inorganic framework around a template molecule, which results in excellent permeability and a uniformly porous structure [26]. In addition, the increased number of active sites on the imprinted sol–gel film enhanced electrochemical signal compared to a monolayer modified electrode [27].

In this paper, we have developed a molecularly imprinted electrochemical sensor for 2-nonylphenol (2-NP) detection utilizing a MIP sol–gel film as a recognition element on a MWNT–NF composite-coated glassy carbon electrode (GCE). The uniform MIP sol–gel film with good adherence and abundant cavities was formed on the transducer surface via surface electrodeposition. MWNT were homogeneously dispersed in Nafion film to improve the MIP immobilisation and enhance the peak current of $K_3Fe(CN)_6$ probe. The electrochemical behavior of $K_3Fe(CN)_6$ on the proposed imprinted sensor was investigated by cyclic voltammetry (CV), differential pulse voltammetry (DPV) and electrochemical impedance spectroscopy (EIS), respectively. This proposed sensor showed excellent sensitivity, selectivity and stability toward analyzing 2-NP. The performance characteristics of the designed sensors were evaluated and the determination of 2-NP was investigated in details.

2. Experimental

2.1. Reagents and solutions

2-NP, *p*-tert-octylpheno (PTOP), bisphnol A (BPA), phenol (PL) were obtained from Alfa Aesar Chemistry Co., Ltd. (Tianjing, China). 3-Aminopropyl triethoxysilane (APTES), phenyltrimethoxysilane (PTMS), tetraethoxysilane (TEOS) were all purchased from Aladdin Chemistry Co., Ltd. (Shanghai, China). Nafion® 1100 suspension (5%, w/w) was acquired from Sigma-Aldrich Co. LLC. (Shanghai, China). MWNT (>95%; diameter: 20–40 nm) were purchased from Shenzhen Nanotech Port Ltd. Co. (Guangdong, China). Ultrapure water obtained from a Millipore water purification system (≥18 MΩ, Milli-Q, Millipore) was used in all assays. All other reagents, including ammonia water, tetrahydrofuran and acetic acid were of analytical grade and were provided by Jinshan Reagent Company (Chengdu, China). Phosphate buffered saline was prepared using 0.2 M Na_2HPO_4 and 0.2 M KH_2PO_4.

2.2. Apparatus

CV and DPV experiments were performed using a conventional three-electrode system, consisting of a bare or modified GCE as the working electrode, a saturated calomel electrode (SCE) as the reference electrode, and a platinum wire as the counter electrode (Shanghai CH Instruments, China). The electrodes were connected to a CHI 660D electrochemistry workstation (Shanghai CH Instruments, China). Surface morphologies of modified electrodes were studied by scanning electron microscopy (SEM) on a Hitachi S-3400N (Japan) microscope. Atomic force microscopy (AFM) images were obtained using a Veeco introduces dimension edge atomic force microscope system (Bruker, USA). EIS experiments were conducted using an Autolab PGSTAT302 electrochemical analyzer (Metrohm, Switzerland) and pH measurements were made with a MP230 pH meter (Mettler, Switzerland).

2.3. Preparation of MIP/sol–gel/MWNT–NF/GCE

The surface of MWNT was grafted with –COOH to enhance dispersion and stability. In our work, 0.5 g crude MWNT was added to 60 mL concentrated HNO_3 under sonication for 10 min. Then the mixture was refluxed under stirring at 85 °C for 12 h. After cooling to room temperature, the mixture was filtered through a 0.22 μm polycarbonate membrane and washed with ultrapure water until the pH of the filtrate reached 7.0. The filtered solid was dried with N_2, and carboxylic acid-functionalized MWNT, denoted as MWNT–COOH, was obtained. Finally, 2.0 mg of MWNT–COOH was dispersed with the aid of ultrasonic agitation in 1.0 mL of 0.5% (w/w) Nafion® in phosphate buffered saline (pH = 7.0) for 1 h to form a homogeneous MWNT–NF suspension solution (2.0 mg mL^{-1}).

Prior to the surface modification, the GCE (3 mm in diameter) was polished to a mirror-like finish with 0.3 and 0.05 μm alumina slurry, and were then successively sonicated in 1:1 (v/v) nitric acid, acetone and ultrapure water. As shown in Scheme 1, surface modification was commenced by applying a 10 μL aliquot solution of the resulting MWNT–NF composite on a GCE and dried at room temperature. To prepare the 2-NP-imprinted sol, 2-NP (2.0 mmol), APTES (2.0 mmol) and PTMS (2.0 mmol) as functional comonomer were dissolved in a 25 mL round-bottomed flask with tetrahydrofuran (5 mL) under magnetic stirring for 30 min. After adding TEOS (8 mmol) and ammonia water (0.8 mL, 0.1 mol L^{-1}) under stirring for 30 min, the mixture was stirred for an additional 2 h before being used as an imprinted sol. Finally, the imprinted sol was electrodesposited on the MWNT–NF/GCE by conducting 30 repetitions of cyclic voltammetry in 5.0 mL of the prepared MIP sol and 5.0 mmol L^{-1} tetrabutylammonium perchlorate between −0.5 and +0.6 V at 50 mV s^{-1}. The electrode was then dried overnight at room temperature. The removal of the 2-NP template was carried out by repeatedly immersing the resultant GCE in a methanol/acetic acid (9:1, v/v) solution for 2 h under continuous agitation and then air-dried for 24 h. The complete removal of 2-NP was verified electrochemically. The finished imprinted electrode was stored at 4 °C in dry condition when not in use. As a control, a non-imprinted polymer (NIP) sensor was prepared and treated in the same manner using the NIP sol.

2.4. Electrochemical measurement

CV and EIS were conducted to characterize the different modified electrodes. The potential of CV was set from −0.3 to +0.6 V with a scan rate of 50 mV s^{-1} and the impedance spectra of frequency range 100 mHz–80 kHz were recorded under a DC potential of 206 mV and an ac voltage of 10 mV amplitude. After being immersed in 2-NP solution for 6 min, the imprinted sensor was carefully washed with distilled water. In DPV, a 50 mV pulse amplitude, a 4 mV potential increment, a 50 ms pulse width and a 200 ms pulse period were used. All electrochemical experiments were conducted at room temperature.

Prior to real-life samples analysis, fresh water samples (obtained from Nanming River, Guiyang, China) were immediately filtered through a millipore cellulose nitrate membrane (pore size was 0.45 μm) to remove suspended particles. The collected wet soil was dried in air and extracted with absolute ethanol for 1 h. After centrifugation, the filtrate was collected and diluted to mark with a phosphate buffered saline (pH = 7.0). Then the pH of all samples were adjusted to 7.0 with phosphate buffered saline.

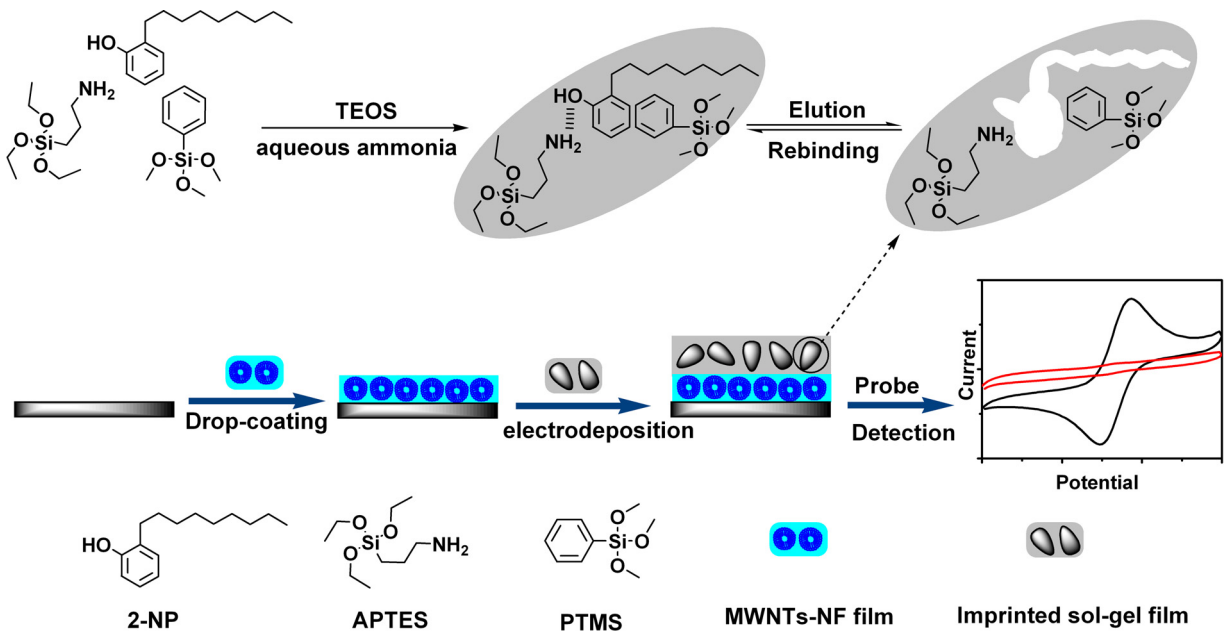

Scheme 1. Schematic representation of the preparation procedure of MIP/sol–gel/MWNT–NF/GCE.

3. Results and discussion

3.1. Preparation and electrochemical behavior of the imprinted sensor

In the sol–gel imprinting process, the amino group of APTES and benzene ring of PTMS can provide recognition sites through hydrogen bonds and "π–π stacking" interaction with the template 2-NP. As a crosslinker, TEOS can form a polymeric network through Si–O bond via hydrolysis. In our work, MIP sol–gel film was deposited on the MWNT–NF/GCE surface by cyclic voltammetry. There were no electrochemical oxidation and reduction arising from the 2-NP template observed within the electrodeposition potential range from −0.5 to +0.6 V, suggesting the 2-NP was not electrochemically active during the electrodeposition process. The electrochemical behavior of the stepwise fabrication process was studied in a pH = 7.0 phosphate buffered saline containing 5 mmol L^{-1} $K_3Fe(CN)_6$, which acts as an electrochemical probe. As shown in Fig. 1A, the cyclic voltammogram of $K_3Fe(CN)_6$ at a bare GCE in trace a shows an oxidation peak at +0.158 V and a reduction peak at +0.251 V. The peak current increased by 401% after MWNTs were immobilised on the electrode (trace b), which is attributed to an increase in effective working electrode surface area by MWNTs. However, compared to MWNTs modified electrode, a 22% decrease in reduction peak current was observed on a MWNT–NF composite modified electrode (trace c). Owing to only a small decrease in the current response observed at the Nafion-modified electrode, Nafion was used in this work as a solubilising agent for MWNT to obtain a homogeneously dispersed imprinted sol–gel recognition film.

Assays were performed to illustrate the imprinting/releasing of 2-NP in the construction process. In Fig. 1B, trace a shows the cyclic voltammogram of $K_3Fe(CN)_6$ at a MIP sol–gel film modified MWNT–NF/GCE. Compared with the CV at a MWNT–NF/GCE shown in Fig. 1A, there was a 99% decrease in the reduction peak current because of difficulty for $K_3Fe(CN)_6$ to penetrate the MIP sol–gel film to make contact with the electrode for electron transfer. Similar responses were detected with the NIP/sol–gel/MWNT–NF/GCE (trace b) due to a lack of selective active sites within the NIP sol gel. However, a significant increase (858%) of the reduction peak current was observed after removing 2-NP from the MIP (trace c). This is most likely due to the formation of channels within a porous MIP without 2-NP, allowing the small $K_3Fe(CN)_6$ to pass through and make contact with the electrode for reduction. In addition, the MWNT–NF composite aided in increasing the electrode surface area, which in turn accelerated the electron transfer reaction at the electrode. After being immersed in 60 μmol L^{-1} 2-NP solution for 6 min (trace d), a 28% decrease in peak current, relative to MIP/sol–gel/MWNT–NF/GCE after extraction of 2-NP, was observed, suggesting the MIP/sol–gel/MWNT–NF/GCE could rebind the target molecules and hinder the probe to arrive at the electrode surface.

Electrochemical impedance spectroscopy (EIS) is a powerful tool for studying the interfacial properties of surface-modified electrodes and the electron-transfer resistance at the electrode surface is an important parameter [28]. In a Nyquist diagram, the semicircle diameter corresponds to the electron-transfer resistance (R_{et}). This resistance affects the electron transfer kinetics of the redox-probe at the electrode interface. The Nyquist diagrams of $K_3Fe(CN)_6$ at different modified electrodes are illustrated in Fig. 2. The high frequency region of trace a (see inset in Fig. 2), which was obtained at a bare GCE, shows an R_{et} (obtained by extrapolation of the semicircles to lower frequencies on the real impedance axis) of 200 Ω. When MWNTs alone (trace b) or an MWNT–NF composite (trace c) was immobilised on the GCE, the R_{et} is 22 Ω and 56 Ω, respectively, indicating the excellent conducting properties of the MWNT–NF composite, which aided in accelerating the electron transfer. Next, R_{et} increased to 3763 Ω at an MIP/sol–gel/MWNT–NF/GCE (trace d), demonstrating the formation of a compact structure by the sol–gel membrane, which then acted as a kinetic barrier for electron transfer. Finally, R_{et} decreased to 2016 Ω after the template was removed (trace e).

3.2. Surface characterization

SEM was performed to obtain an insight into the surface morphology of these various modified electrodes. As shown in Fig. 3A, high-density large intertwined aggregates were observed and the arrangement was chaotic and irregular. Fig. 3B displays a SEM image of MWNT dispersed in the Nafion solution. Well-separated

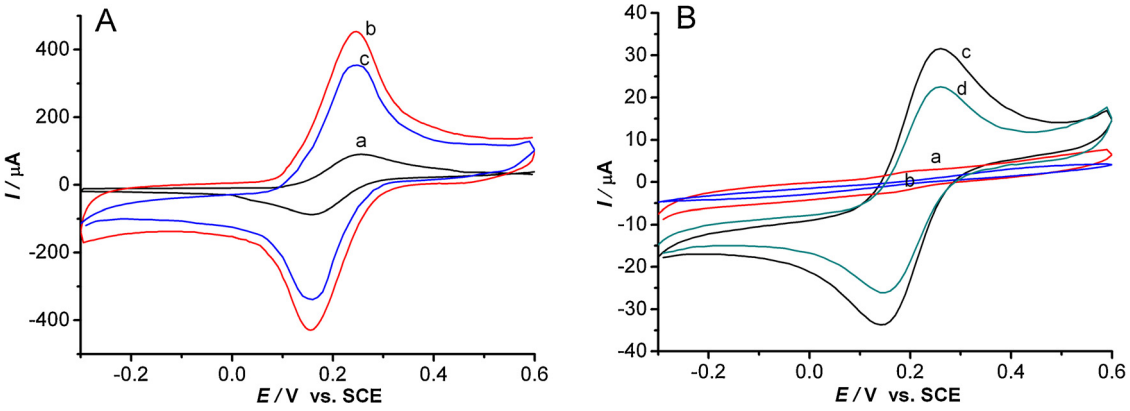

Fig. 1. (A) CV of $K_3Fe(CN)_6$ on the bare GCE (a), MWNT/GCE (b) and MWNT–NF/GCE (c); (B) CV of $K_3Fe(CN)_6$ on the MIP/sol–gel/MWNT–NF/GCE (a), NIP/sol–gel/MWNT–NF/GCE (b), MIP/sol–gel/MWNT–NF/GCE after extraction of 2-NP (c) and rebinding in 60 μmol L^{-1} 2-NP (d) in 0.1 mol L^{-1} phosphate buffered saline (pH = 7.0) consisting of 5 mmol L^{-1} of $K_3Fe(CN)_6$ and 0.1 mol L^{-1} of KCl.

MWNT rope are detectable on the surface of MWNT–NF/GCE. We have also examined surface morphology using AFM, which enables characterisation of nanoparticles at ambient conditions [29]. Accordingly, the AFM image of MWNT particles is shown in the inset of Fig. 3B, revealing a rope shape with slightly rough surface. After electrodeposition of the imprinted sol, it can be visualized from Fig. 3C that the average size of MIP sol–gel/MWNT particles (Fig. 3C inset) increasing obviously compared with MWNT particles (Fig. 3B inset), as well as embedded throughout the polymer matrix, suggesting that the MIP sol–gel was attached on the MWNT successfully. The MIP/sol–gel/MWNT/GCE surface (Fig. 3D) appears rather conglomerate compared to MIP/sol–gel/MWNT–NF/GCE surface (Fig. 3C), indicating that the Nafion plays a key role in preparing a homogeneous and well-distributed MIP sol–gel film.

3.3. Optimization of the parameters of imprinted sensor

Three MIP sol–gel films consisting of (i) APTES alone as the monomer, (ii) PTMS alone as the monomer and (iii) both APTES and PTMDS as co-monomers were used to fabricate imprinted sensors with optimum sensing properties and high binding capacity of 2-NP. The respective imprinted sensors will thereafter be denoted as A-MIP/sol–gel/MWNT–NF/GCE, P-MIP/sol–gel/MWNT–NF/GCE, and AP-MIP/sol–gel/MWNT–NF/GCE. The response performance of

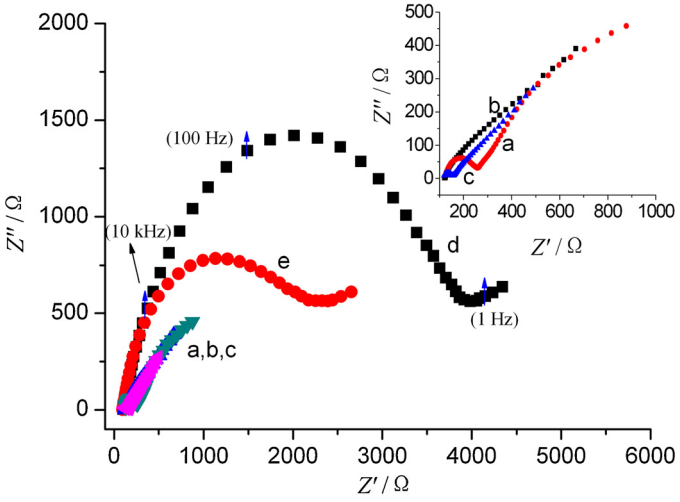

Fig. 2. Electrochemical impedance spectroscopy of bare GCE (a), MWNT/GCE (b), MWNT–NF/GCE (c), MIP/sol–gel/MWNT–NF/GCE before (d) and after (e) leaching 2-NP in 5 mmol L^{-1} of $K_3Fe(CN)_6$ containing of 0.1 mol L^{-1} KCl. The inset shows the amplified EIS of curve a, b and c.

the three sensors are investigated and the results are shown in Fig. 4A. The current variation (ΔI) ($\Delta I = I_c - I_0$, where I_0 refers to the current signal obtained in a blank solution, and I_c denotes the corresponding current signal in a solution of concentration c μmol L^{-1}) of AP-MIP/sol–gel/MWNT–NF/GCE (chart b) was higher than that at a P-MIP/sol–gel/MWNT–NF/GCE (chart a) and at an A-MIP/sol–gel/MWNT–NF/GCE (chart c). This indicates that the combined utilization of APTES and PTMS generates highly selective cavities and provides stronger interaction forces, such as π–π stacking or hydrogen bonding, for 2-NP compared to those found in imprinted sensors consisting of APTES or PTMA alone. Therefore, APTES and PTMS as the functional co-monomers would contribute the imprinting effect of the polymer matrix thus prepared.

The influence of the test solution pH on the peak current of $K_3Fe(CN)_6$ at the MIP/sol–gel/MWNT–NF/GCE was investigated by DPV over the range from 4.0 to 10.0. As illustrated in Fig. 4B, the ΔI of $K_3Fe(CN)_6$ at the imprinted electrode increased rapidly with the increasing pH from 4.0 to 7.0. Then, it decreased when the pH value exceeded 8.0, and the highest ΔI was obtained at pH = 7.0, suggesting that this pH of external solution would facilitate the interaction between 2-NP and the imprinted film containing functional groups. The pH of the solution affects the degree of ionization of 2-NP (pK_a = 10.7) and the protonation of functional monomer, which subsequently leads to a change in electrostatic binding of 2-NP in MIP cavities [22]. The neutral and non-ionised 2-NP is much better for the recognition process. Therefore, a pH value of 7.0 was chosen as the optimized external solution pH for the subsequent analytical experiments.

Fig. 4C shows the dependence of the sensor response on the incubation time ranging from 1 to 10 min, using a fixed 2-NP concentration of 60 μmol L^{-1}. The reduction peak current initially increased steadily but reached 95% of the saturated adsorption within 5 min of incubation, before it slowly levelled off, indicating a rapid recognition capability of the imprinted film and its high affinity to the target molecule. The stable current response of MIP/sol–gel/MWNT–NF/GCE was obtained in about 6 min, so the incubation time of 6 min was implemented in subsequent experiments.

3.4. Performance of the imprinted sensor

3.4.1. Linear range and limit of detection

A series of different concentrations of 2-NP solutions were measured with the imprinted sensor to investigate linear range and limit of detection. As shown in Fig. 5, with the 2-NP concentration increased, the reduction peak current of $K_3Fe(CN)_6$ at

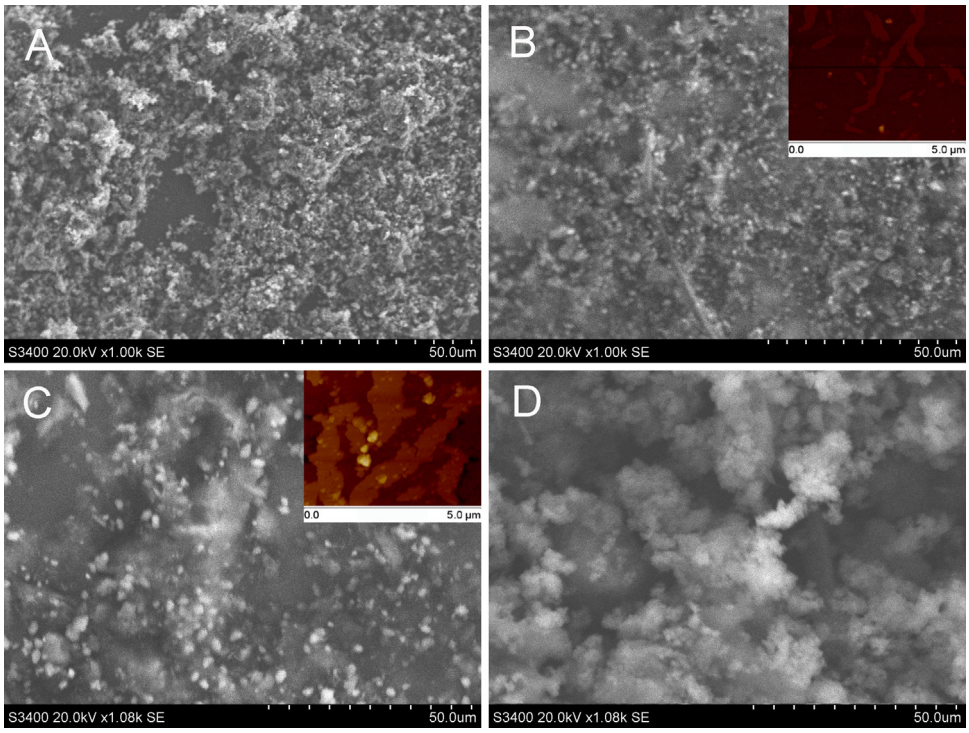

Fig. 3. SEM images of (a) MWNT/GCE, (b) MWNT–NF/GCE, (c) MIP/sol–gel/MWNT–NF/GCE and (d) MIP/sol–gel/MWNT/GCE surface. The inset shows the AFM images of (b) MWNT and (c) MIP/sol–gel/MWNT particles.

the MIP/sol–gel/MWNT–NF/GCE gradually decreased. Under optimized conditions, the proposed sensor showed a linear response in the range from 0.2 to 360 μmol L^{-1}, described by the equation: $i(\mu A) = -0.084$ [2-NP] (μmol L^{-1}) +45.69 ($r^2 = 0.9918$, $n = 5$), with a relative standard deviation (RSD) lower than 3.5%. The detection limit, estimated as the 2-NP concentration yielding an amperometric signal equal to three times the peak-to-peak noise of the baseline, was 0.06 μmol L^{-1}. Compared with other electrochemical sensors for 2-NP (Table 1) reported in literature [11,30], the proposed sensor provided with a wider linear range. More importantly, the limit of detection was lower than that (0.32 μmol L^{-1}) estimated at an 2-NP imprinted electrochemical sensor consisting of titanium oxide and gold nanomaterials [31], and was comparable to 0.058 μmol L^{-1} reported by Meng et al. [10] and 0.01 μmol L^{-1} by Lu et al. [30].

3.4.2. Stability and repeatability

The stability and repeatability of the MIP/sol–gel/MWNT–NF/GCE were studied by DPV measurements of 60 μmol L^{-1} 2-NP and the results are presented in Fig. 6. The peak current retained 90.3% of its initial current after 30 days storage in phosphate buffered saline at 4 °C and measured intermittently (every 5 days), indicating a satisfactory stability of the sensor in this experiment. The RSD of the MIP/sol–gel/MWNT–NF/GCE was 3.6% for 20 successive measurements, and lower than 6.4% for measuring at intervals of 2 days in 30 days period, respectively, indicating acceptable fabrication repeatability.

3.5. Selectivity of the imprinted sensor

We have studied the electrochemical response of MIP and NIP modified electrodes with different concentration of 2-NP. As seen from Fig. 7A, the MIP modified electrode showed larger ΔI than the NIP modified electrode, with an imprinting factor (*IF*) value of 6.47 ($IF = \Delta f_{MIP}/\Delta f_{NIP}$, where Δf_{MIP} and Δf_{NIP} are the slope of the calibration plot for different concentrations of analytes on MIP/sol–gel/MWNT–NF/GCE and NIP/sol–gel/MWNT–NF/GCE, respectively), suggesting a successful imprinting process and 2-NP interacted with the specific binding sites within the MIP materials, whereas it interacted non-specifically with NIP. In order

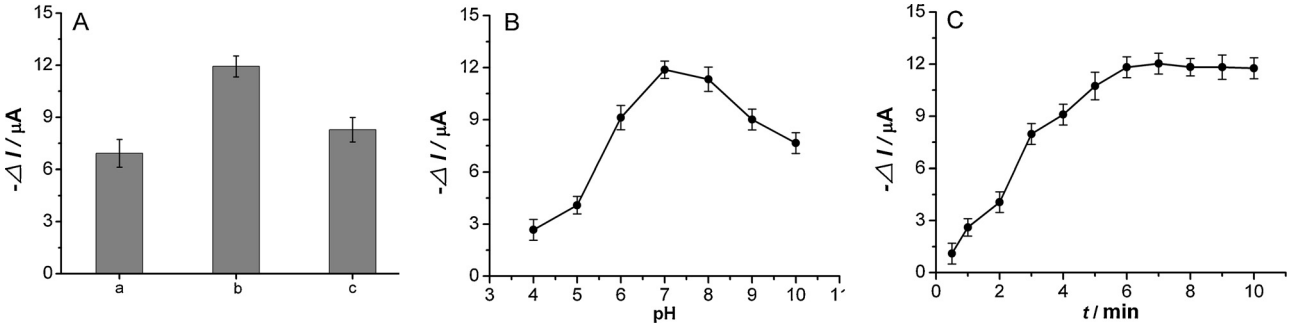

Fig. 4. Effects of (A) the type of functional monomer (a) PTMS, (b) APTES and PTMS, and (c) APTES; (B) pH and (C) immersion time on the current variation (ΔI) using the proposed sensor. Background electrolyte: 0.1 mol L^{-1} phosphate buffered solutions of pH = 7.0 containing 5 mmol L^{-1} of $K_3Fe(CN)_6$ and 0.1 mol L^{-1} KCl. [2-NP] = 60 μmol L^{-1}.

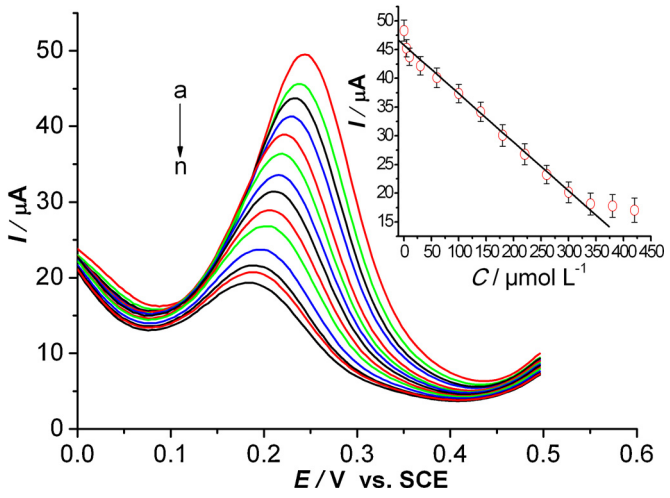

Fig. 5. DVP curves for 2-NP detection using the proposed sensor in 0.1 mol L^{-1} phosphate buffered saline (pH = 7.0) containing 5 mmol L^{-1} of $K_3Fe(CN)_6$ and 0.1 mol L^{-1} of KCl. vs.SCE. [2-NP] = 0.2,5,10,30,60,100,140,180,220,260,300, 340,380,420 μmol L^{-1} (from a to n). The inset is a plot of the linear relationship between the peak current and the concentration of 2-NP.

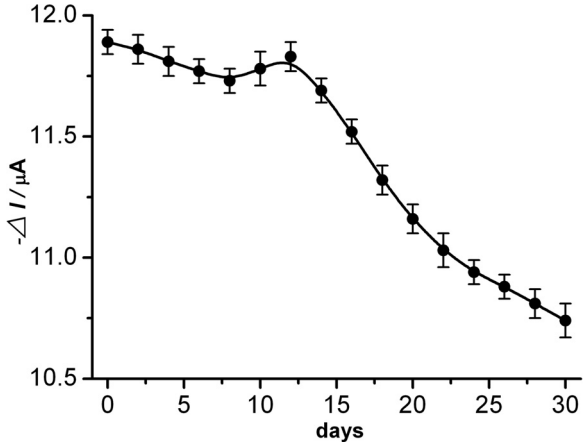

Fig. 6. Reproducibility and stability of the MIP/sol–gel/MWNT–NF/GCE measured by 30 days period.

to ensure selectivity of the imprinted sensor, DPV responses of 2-NP and structural analogs including PTOP, BPA and PL on MIP/sol–gel/MWNT–NF/GCE were compared and the results are shown in Fig. 7B. Notably, the MIP modified electrode exhibited a much higher current response toward 2-NP compared with the structural analogues. No perceivable difference of current variation, however, was observed for the analogues, showing that MIP sol–gel had the highest specific selectivity toward 2-NP. The origin of selective recognition can be attributed to 2-NP selective binding sites in the polymer sol–gel created by the imprinting process. Although the same hydrogen bond can form between the structural analogues and the monomer, the different recognition effect may be based on the distinct size, structure and functional group to the template [32]. Moreover, PL has minimal obstruction to approach the recognition cavities because its smaller molecular structure, showed a bigger current response than other structural analogues, but it was still much lower than that for 2-NP, suggesting that the memory of specific functional group also plays an important role in the conformation memory [33]. These results suggested that the imprinting process significantly improved affinity and selectivity of the 2-NP imprinted sol–gel toward template 2-NP.

3.6. Preliminary analysis of 2-NP in environmental samples

The practical applicability of the proposed sensor was examined by analyzing the 2-NP in environmental water samples from three different sources including tap water, river water, and soil samples (collected from Guiyang, China) under optimized conditions. As no 2-NP was found in the samples, the accuracy of the method was evaluated by performing a recovery test after spiking the samples. As shown in Table 2, the recoveries ranged from 95.4 to 98.1% and RSD was from 2.5% to 4.4%, suggesting an acceptable detection result and the viability in using the proposed sensor for 2-NP analysis in these real-life samples.

4. Conclusions

In this work, a simple, rapid, sensitive and selective molecularly imprinted electrochemical sensor for 2-NP detection based on electrodepositing MIP sol–gel onto an MWNT–NF composite modified GCE was described. Nafion was selected to improve on the dispersibility of MWNT for preparing a homogeneous and well-distributed MIP sol–gel film. The developed sensor provided with a wider linear range and lower limit of detection compared with other 2-NP electrochemical sensors. In addition, it displayed a good

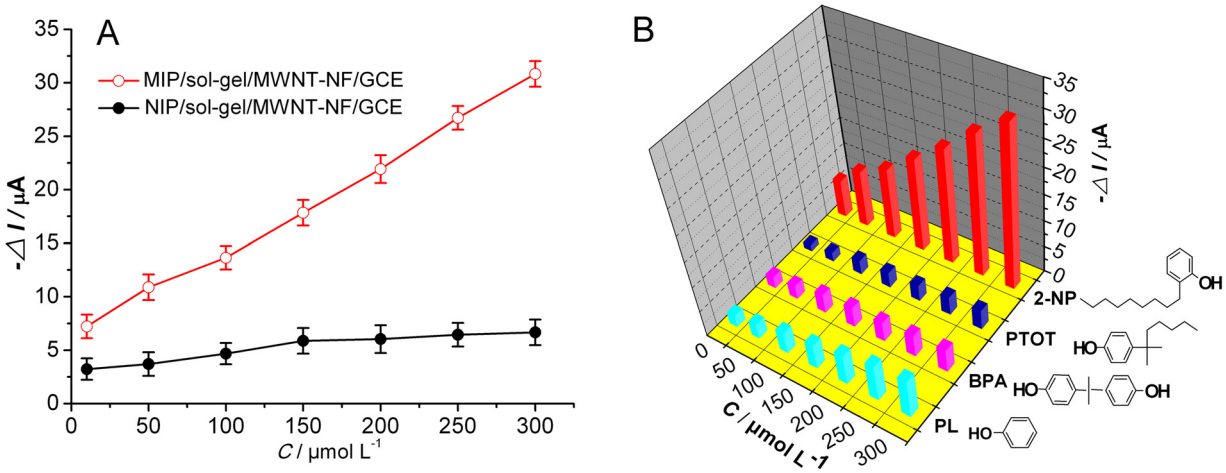

Fig. 7. (A) Calibration plots of current response changes corresponding to the MIP/sol–gel/MWNT–NF/GCE and NIP/sol–gel/MWNT–NF/GCE for different concentrations of 2-NP, respectively; (B) MIP/sol–gel/MWNT–NF/GCE response for different concentrations of 2-NP, PTOP, BPA and PL, respectively.

recognition capacity for 2-NP in the presence of several phenol structural analogs including PTOP, BPA and PL and showed good stability and repeatability. More importantly, the proposed sensor has successfully been applied to detection of 2-NP in real-life samples and had shown a great potential use in the environmental samples analysis.

Acknowledgments

This work was financially supported by the Natural Science Foundation of education department of Guizhou Province (No. 2010054), the Natural Science Foundation of Guizhou Province (No. J20102120), and the Key Disciplines Construction Foundation of Guizhou Province (No. 2012442).

References

[1] S. Frassinetti, C. Barberio, L. Caltavuturo, F. Fava, D. Di Gioia, Genotoxicity of 4-nonyl-phenol and nonylphenol ethoxylate mixtures by the use of *Saccharomyces cerevisiae* D7 mutation assay and use of this text to evaluate the efficiency of biodegradation treatments, Ecotoxicol. Environ. Saf. 74 (2011) 253–258.
[2] H. Kuramitz, J. Saitoh, T. Hattori, S. Tanaka, Electrochemical removal of *p*-nonylphenol from dilute solutions using a carbon fiber anode, Water Res. 36 (2002) 3323–3329.
[3] A. Soares, B. Guieysse, B. Jefferson, E. Cartmell, J. Lester, Nonylphenol in the environment: a critical review on occurrence, fate, toxicity and treatment in wastewaters, Environ. Int. 34 (2008) 1033–1049.
[4] S.H. Lee, H.M. Woo, B.H. Jung, J. Lee, O.S. Kwon, H.S. Pyo, M.H. Choi, B.C. Chung, Metabolomic approach to evaluate the toxicological effects of nonylphenol with rat urine, Anal. Chem. 79 (2007) 6102–6110.
[5] D. Bonenfant, P. Niquette, M. Mimeault, A. Furtos-Matei, R. Hausler, UV–VIS and FTIR spectroscopic analyses of inclusion complexes of nonylphenol and nonylphenol ethoxylate with [beta]-cyclodextrin, Water Res. 43 (2009) 3575–3581.
[6] A. Díaz, L. Vàzquez, F. Ventura, M.T. Galceran, Estimation of measurement uncertainty for the determination of nonylphenol in water using solid-phase extraction and solid-phase microextraction procedures, Anal. Chim. Acta 506 (2004) 71–80.
[7] K. Inoue, Y. Yoshimura, T. Makino, H. Nakazawa, S. Affiliations, H. Affiliations, Determination of 4-nonylphenol and 4-octylphenol in human blood samples by high-performance liquid chromatography with multi-electrode electrochemical coulometric-array detection, Analyst 125 (2000) 1959–1961.
[8] T. Raecker, B. Thiele, R.M. Boehme, K. Guenther, Endocrine disrupting nonyl-and octylphenol in infant food in Germany: considerable daily intake of nonylphenol for babies, Chemosphere 82 (2011) 1533–1540.
[9] G.A. Evtugyn, S.A. Eremin, R.P. Shaljamova, A.R. Ismagilova, H.C. Budnikov, Amperometric immunosensor for nonylphenol determination based on peroxidase indicating reaction, Biosens. Bioelectron. 22 (2006) 56–62.
[10] X. Meng, H. Yin, M. Xu, S. Ai, J. Zhu, Electrochemical determination of nonylphenol based on ionic liquid-functionalized graphene nanosheet modified glassy carbon electrode and its interaction with DNA, J. Solid State Electrochem. 16 (2012) 837–2843.
[11] A.B. Albadarin, C. Mangwandi, A.H. Al-Muhtaseb, G.M. Walker, S.J. Allen, M.N.M. Ahmad, Kinetic and thermodynamics of chromium ions adsorption onto low-cost dolomite adsorbent, Chem. Eng. J. 179 (2012) 193–202.
[12] C. Malitesta, E. Mazzotta, R.A. Picca, A. Poma, I. Chianella, S.A. Piletsky, MIP sensors—the electrochemical approach, Anal. Bioanal. Chem. 402 (2012) 1827–1846.
[13] X.G. Hu, J.L. Pan, Y.L. Hu, Y. Huo, G.K. Li, Preparation and evaluation of solid-phase microextraction fiber based on molecularly imprinted polymers for trace analysis of tetracyclines in complicated samples, J. Chromatogr. A 1188 (2008) 97–107.
[14] X.L. Xu, G.L. Zhou, H.X. Li, Q. Liu, S. Zhang, J.L. Kong, A novel molecularly imprinted sensor for selectively probing imipramine created on ITO electrodes modified by Au nanoparticles, Talanta 78 (2009) 26–32.
[15] X.W. Kan, Y. Zhao, Z.R. Geng, Z.L. Wang, J.J. Zhu, Composites of multiwalled carbon nanotubes and molecularly imprinted polymers for dopamine recognition, J. Phys. Chem. C 112 (2008) 4849–4854.
[16] H. Lee, S.W. Yoon, E.J. Kim, J. Park, In-situ growth of copper sulfide nanocrystals on multiwalled carbon nanotubes and their application as novel solar cell and amperometric glucose sensor materials, Nano Lett. 7 (2007) 778–784.
[17] J. Li, F. Jiang, X. Wei, Molecularly imprinted sensor based on an enzyme amplifier for ultratrace oxytetracycline determination, Anal. Chem. 82 (2010) 6074–6078.
[18] C. Xie, H. Li, S. Li, J. Wu, Z. Zhang, Surface molecular self-assembly for organophosphate pesticide imprinting in electropolymerized poly (*p*-aminothiophenol) membranes on a gold nanoparticle modified glassy carbon electrode, Anal. Chem. 82 (2009) 241–249.
[19] J. Zhang, Y.Q. Wang, R.H. Lv, L. Xu, Electrochemical tolazoline sensor based on gold nanoparticles and imprinted poly-*o*-aminothiophenol film, Electrochim. Acta 55 (2010) 4039–4044.
[20] S. Suriyanarayanan, P.J. Cywinski, A.J. Moro, G.J. Mohr, W. Kutner, Chemosensors based on molecularly imprinted polymers, Top. Curr. Chem. 325 (2012) 165–266.
[21] P.S. Sharma, A. Pietrzyk-Le, F. D'Souza, W. Kutner, Electrochemically synthesized polymers in molecular imprinting for chemical sensing, Anal. Bioanal. Chem. 402 (2012) 3177–3204.
[22] B. Prasad, D. Kumar, R. Madhuri, M.P. Tiwari, Sol–gel derived multiwalled carbon nanotubes ceramic electrode modified with molecularly imprinted polymer for ultra trace sensing of dopamine in real samples, Electrochim. Acta 56 (2011) 7202–7211.
[23] S.A. Kumar, S.F. Wang, C.T. Yeh, H.C. Lu, J.C. Yang, Y.T. Chang, Direct electron transfer of cytochrome *C* and its electrocatalytic properties on multiwalled carbon nanotubes/ciprofloxacin films, J. Solid State Electrochem. 14 (2010) 2129–2135.
[24] J.R.M. Neto, W.J.R. Santos, P.R. Lima, A hemin-based molecularly imprinted polymer (MIP) grafted onto a glassy carbon electrode as a selective sensor for 4-aminophenol amperometric, Sens. Actuators, B 152 (2011) 220–225.
[25] J. Wang, M. Musameh, Y. Lin, Solubilization of carbon nanotubes by Nafion toward the preparation of amperometric biosensors, J. Am. Chem. Soc. 125 (2003) 2408–2409.
[26] Y. Yang, G. Fang, G. Liu, M. Pan, X. Wang, L. Kong, X. He, S. Wang, Electrochemical sensor based on molecularly imprinted polymer film via sol–gel technology and multi-walled carbon nanotubes-chitosan functional layer for sensitive determination of quinoxaline-2-carboxylic acid, Biosens. Bioelectron. 47 (2013) 475–481.
[27] N.R. Walker, M.J. Linman, M. Timmers, S.L. Dean, C.M. Burkett, J.A. Lloyd, J.D. Keelor, B.M. Baughman, P.L. Edmiston, P.L. Edmiston, Selective detection of gas-phase TNT by integrated optical waveguide spectrometry using molecularly imprinted sol–gel sensing films, Anal. Chim. Acta 593 (2007) 82–91.
[28] L. Alfonta, E. Katz, I. Willner, Sensing of acetylcholine by a tricomponent-enzyme layered electrode using faradaic impedance spectroscopy, cyclic voltammetry, and microgravimetric quartz crystal microbalance transduction methods, Anal. Chem. 72 (2000) 927–935.
[29] S. Yaqub, U. Latif, F.L. Dickert, Plastic antibodies as chemical sensor material for atrazine detection, Sens. Actuators, B 160 (2011) 227–233.
[30] Q. Lu, W. Zhang, Z. Wang, G. Yu, Y. Yuan, Y. Zhou, A Facile Electrochemical sensor for nonylphenol determination based on the enhancement effect of cetyltrimethylammonium bromide, Sensors 13 (2013) 758–768.
[31] J. Huang, X. Zhang, S. Liu, Q. Lin, X. He, X. Xing, Development of molecularly imprinted electrochemical sensor with titanium oxide and gold nanomaterials enhanced technique for determination of 4-nonylphenol, Sens. Actuators, B 152 (2011) 292–298.
[32] Y. Chang, T. Ko, T. Hsu, M. Syu, Synthesis of an imprinted hybrid organic–inorganic polymeric sol–gel matrix toward the specific binding and isotherm kinetics investigation of creatinine, Anal. Chem. 81 (2009) 2098–2105.
[33] Z.Y. Chen, Z.D. Hua, J. Wang, Y. Guan, M.P. Zhao, Y.Z. Li, Molecularly imprinted soluble nanogels as a peroxidase-like catalyst in the oxidation reaction of homovanillic acid under aqueous conditions, Appl. Catal., A 328 (2007) 252–258.

Biographies

Jin Zhang obtained his M.S. in 2010 from Southwest University, China. He is an associate professor at School of Chemistry and Life Science, Guizhou Normal College. Currently he is a Ph.D. candidate in Chinese Academy of Sciences. His major research interests include electrochemical sensors and environmental analytical chemistry.

Yan-Hui Niu obtained her M.S. in 2008 from Shanxi Normal University, China. She is an associate professor at School of Chemistry and Life Science, Guizhou Normal College. Her research interest is electrochemical sensors.

Shi-Jie Li is a professor at Institute of Geochemistry, Chinese Academy of Sciences. He obtained his Ph.D. in 1993 from Chinese Academy of Sciences. His research focuses on Lake Sediment and Environmental Analysis.

Rong-Qin Luo is Ph.D. candidate in Chinese Academy of Sciences. Her major research interest is environmental analytical chemistry.

Chao-Ying Wang is a professor of analytical chemistry at School of Chemistry and Life Science, Guizhou Normal College. Her research focuses on molecular spectroscopy, electroanalytical chemistry and environmental analytical chemistry.